Title

Isoproterenol-Induced Cardiac Diastolic Dysfunction in Mice: A Systems Genetics Analysis.

Permalink

https://escholarship.org/uc/item/41d8k7jg

Authors

Wang, Jessica

Huertas-Vazquez, Adriana

Wang, Yibin

et al.

Publication Date

2019

DOI

10.3389/fcvm.2019.00100

Peer reviewed

Isoproterenol-Induced Cardiac Diastolic Dysfunction in Mice: A Systems Genetics Analysis

Jessica Wang[1]*, Adriana Huertas-Vazquez[1], Yibin Wang[2] and Aldons J. Lusis[1]

[1] Department of Medicine, University of California, Los Angeles, Los Angeles, CA, United States, [2] Department of Anesthesiology, University of California, Los Angeles, Los Angeles, CA, United States

We examined an isoproterenol heart failure model across a panel of diverse inbred strains of mice, the Hybrid Mouse Diversity Panel (HMDP), using left atrial (LA) and lung weights as well as echocardiogram parameters as surrogates for cardiac diastolic function. We identified gene transcripts that significantly correlated with diastolic function. In addition, we mapped echocardiographic parameters associated with diastolic function. We identified a locus near *Tns3-Hus1* to be associated with baseline E/A ratio in mice ($p = 1.65E-06$), the syntenic region of which was recently associated with E/A ratio in a genome-wide association study (GWAS) meta-analysis of the EchoGen consortium in humans. We also identified a locus near *Cdkn2a-Cdkn2b*, which is a region syntenic to the human 9p21 locus, to be associated with week 3 A/E ratio ($p = 2.15E-06$). Our study is the first study to map diastolic dysfunction in mice, in which a locus was found to be shared with a recent human GWAS on diastolic function. Moreover, our cardiac transcriptome correlation and eQTL analysis generated hypotheses for future basic investigations. These results showed that, although technical and physiological challenges limit diastolic function assessment in mice and humans, future investigations examining the genetic architecture of diastolic function among a diverse mouse population, such as the HMDP, in controlled experimental settings, offer distinct advantages in understanding the genetic determinants of diastolic function.

Keywords: diastolic function, genome-wide association, isoproterenol, mouse, gene expression

INTRODUCTION

Heart failure with preserved ejection fraction (HFpEF) is a clinical syndrome that is characterized by diastolic dysfunction, involving impaired relaxation and compliance of the left ventricle (LV), leading to increased LV filling pressures, heart failure symptoms and an elevated risk of mortality (1–4). Among 5.7 million Americans with heart failure, HFpEF accounts for 50% of all heart failure hospital admissions (5). Although the understanding of HFpEF pathophysiology and risk factors, such as older age, female sex, hypertension, metabolic syndrome, renal dysfunction and obesity, has improved, treatment aimed at altering its natural history has yet to be developed due to the lack of understanding of its molecular underpinnings (6).

The Hybrid Mouse Diversity Panel (HMDP) consists of ∼100 well-characterized inbred mouse strains that can be used to study genetic and environmental factors underlying complex traits (7). The HMDP, with a fully annotated genome and an easily controlled environment, can be readily manipulated to create a disease model for in-depth multi-omics molecular characterization at the

tissue level. We had previously reported isoproterenol-induced cardiac phenotypes in the HMDP, in which we identified and validated a number of genomic loci associated with systolic heart failure traits via a genome-wide association approach (8–10). Chronic isoproterenol administration in mice has previously been demonstrated to induce diastolic dysfunction, as shown by an upward shift of the pressure-volume relationship (11). Although diastolic function can be assessed by directly measuring LV filling pressures via invasive hemodynamic monitoring (12), it can also be assessed by a number of echocardiographic findings non-invasively. These parameters, E and A velocities, tissue E' velocity, and their derivatives E/A ratio and E/E' ratio, have been used to study diastolic function in mice (13). The present study focuses on diastolic function data and analyses that have not been previously published. In this study we analyzed diastolic function parameters from the heart failure HMDP to identify candidate genomic loci and gene transcripts that may more accurately reflect the pathophysiology of diastolic dysfunction. Finally, we hypothesize the use of a diverse mouse population, such as the HMDP, to help us better understand diastolic dysfunction.

METHODS

Assessment of Diastolic Function in Mice

Female mice at a median age of 9 weeks from 104 of the HMDP inbred strains were treated with isoproterenol (30 mg/kg/d) via an intra-abdominally implanted osmotic pump for 21 days as previously described (8–10). Briefly, baseline (prior to isoproterenol pump implantation), week 1, week 2, and week 3 echocardiograms were obtained. Due to tissue E' and A' velocities not being available on the VisualSonics Vevo 770 ultrasonography system used for this study, diastolic function was assessed by E and A velocities and via left atrial and lung weights. At the end of the protocol, heart chambers and organs were dissected and weighed. Left ventricular tissue was frozen in liquid nitrogen and later prepared for gene expression profiling as previously described (8–10).

GWAS and Correlation Analysis

The HMDP mouse strains were previously genotyped using the JAX Mouse Diversity Genotyping Array (14). Mapping of diastolic function traits was performed using the Factored Spectrally Transformed Linear Mixed Models (FaST-LMM) as previously described (15). Gene-trait correlation analyses were performed using WGCNA (16). Additional details of the methods were previously described (8–10). The threshold for genome-wide significance in mice was previously determined through simulation and permutation of strain genotypes in the hybrid mouse diversity panel to be 4.1×10^{-6} by Farber et al. The significance threshold for local expression quantitative trait loci (eQTL) was similarly determined to be 3.63×10^{-3}. In our exam of multiple related diastolic function traits, the genome-wide significance threshold for each clinical trait was kept at the nominal p-value of 4.1×10^{-6} without further Bonferroni adjustment to account for each trait tested. We applied the Benjamini-Hochberg (BH) procedure with a false discovery rate of 5% to account for multiple testing in trait-expression correlation analysis.
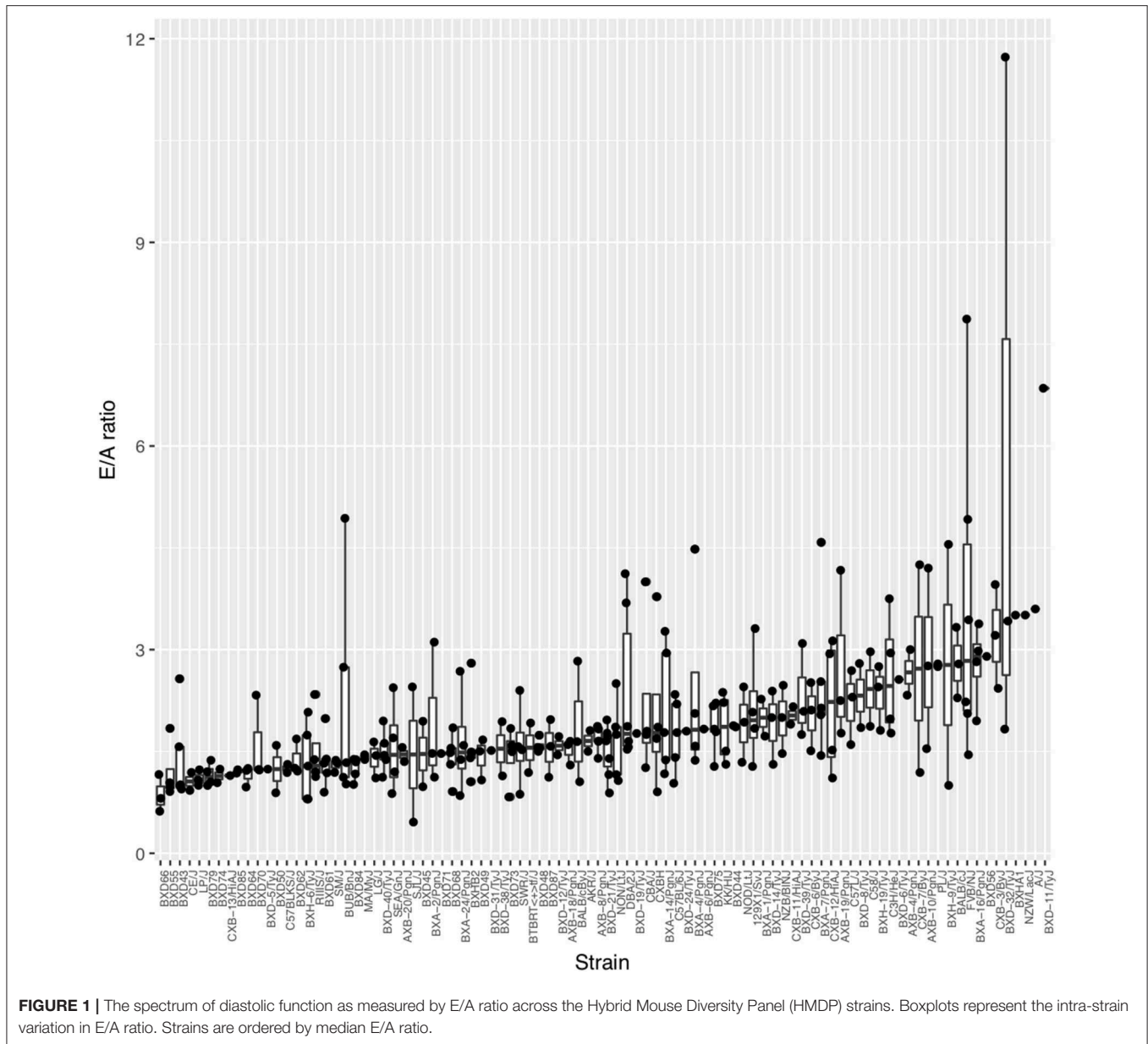
RESULTS

One-hundred and four classical and recombinant inbred mouse strains of the HMDP underwent intraperitoneal implantation of isoproterenol mini-pumps. Global gene expression of the left ventricular tissue was performed as previously reported (8–10). Diastolic function was assessed by echocardiographic measures, such as E and A velocities, and left atrial and lung weights, which reflect cumulative impact of isoproterenol on LV filling pressures over time, leading to atrial volume increase, pulmonary congestion, and edema (17). Tissue velocity measurement was not available on the ultrasonography system used for the study.

Diastolic Function Assessment Across the HMDP Population

On average across the HMDP strains, left atrial weight at the time of sacrifice had increased by 78.8% among isoproterenol treated vs. control mice (4.29 ± 1.69 mg vs. 2.4 ± 0.583 mg; p = 9.33E-20), indicating significant left atrial remodeling due to isoproterenol-induced elevated filling pressures over 3 weeks (**Supplementary Table 1A**). Of note, ejection fraction (EF) did not change on average between baseline and week 3 of isoproterenol. These findings are consistent with an isoproterenol-induced HFpEF model on average among HMDP mice. In terms of echocardiographic measures of diastolic function, average E and A velocities increased with isoproterenol during the first week and, thereby, remained relatively unchanged for the rest of isoproterenol treatment (**Supplementary Table 2**). E/A ratio did not change significantly on average (**Supplementary Table 1B**). There was a wide distribution of E/A ratio among HMDP strains at week 3 of isoproterenol with only a minority of strains with E/A ratio < 1, indicating varying degrees of diastolic dysfunction (**Figure 1**). There is no significant correlation between E/A and fibrosis (**Supplementary Figure 1**), indicative of intrinsic relaxation properties rather than extracellular fibrotic processes as the primary driver of the E/A ratio phenotype.

Diastolic Function Correlation With Left Ventricular Gene Transcripts

We examined isoproterenol-treated transcripts that were most significantly correlated with diastolic function traits such as left atrial weight, lung weight, E and A velocities (**Table 1**). Many of the significantly correlated gene transcripts have been reported to be expressed in the heart but their specific roles in heart failure have not been previously explored. A few of the notable gene transcripts with known roles in the heart are described as follows. *Adamts2*, which was significantly correlated with lung weight (r = 0.459, p = 5.49e−06), has been previously reported by our group to be a driver of cardiac hypertrophy (8) and confirmed by another group using gain- and loss-of-function genetic mouse model of *Adamts2* to negatively regulate cardiomyocyte hypertrophy via the PI3K/AKT-dependent signaling pathway

FIGURE 1 | The spectrum of diastolic function as measured by E/A ratio across the Hybrid Mouse Diversity Panel (HMDP) strains. Boxplots represent the intra-strain variation in E/A ratio. Strains are ordered by median E/A ratio.

(18). *Vav2*, which was correlated with E velocity at week 3 (r = 0.469, p = 4.12e−06), is a signal transduction molecule that activates Rho/Rac GTPases, the knockout of which in mice causes tachycardia, hypertension, defects in the heart, arterial walls and kidneys via chronic stimulation of the renin/angiotensin II and sympathetic nervous systems (19). *Tmod4*, a muscle-specific member of the tropomodulin family of actin-regulatory proteins (20), was found to be negatively correlated with left atrial weight (r = −0.466, p = 3.69e−06). Moreover, *Jmjd1a*, a histone 3 lysine 9 (H3K9)-specific demethylase that binds all 3 myocardin family members, was positively correlated with A velocity at week 3 with borderline significance (r = 0.457, p = 7.69e−06, BH adjusted p = 0.0549) and is known to be upregulated in myocardium from patients with hypertrophic heart disease (21). Finally, *Col6a1*, which was correlated with lung weight with

borderline significance (r = 0.451, p = 7.95e−06, BH adjusted p = 0.0549) has previously been shown, when absent, to be protective following myocardial infarction by limiting infarct size, apoptosis, aberrant remodeling and fibrosis (22).

Genome-Wide Association of Diastolic Function Parameters Across the HMDP Population

Assuming that diastolic function cannot be normal under continuous beta-adrenergic stimulation by isoproterenol over 3 weeks, E/A ratio measurements may be treated as a monotonic continuous variable, where the higher the value the more diastolic dysfunction there is. This assumption obviates the need to distinguish normal vs. pseudonormal

TABLE 1 | Significantly correlated isoproterenol-induced transcripts with diastolic function parameters including left atrial weight, lung, E and A velocity and E/A ratio.

|	Gene symbol	Probe ID	Phenotype	Pearson correlation	P-value	Adjusted p-value
1	Stx16	ILMN_2735822	E velocity	0.513	3.26E-07	0.019
2	Ms4a4d	ILMN_2735547	E velocity	0.500	7.13E-07	0.025
3	Vav2	ILMN_1223067	E velocity	0.469	4.12E-06	0.044
4	Galr3	ILMN_2887408	LA weight	0.561	9.08E-09	0.005
5	Olfr1306	ILMN_3162277	LA weight	0.526	1.01E-07	0.013
6	Nrip3	ILMN_2875404	LA weight	0.516	2.00E-07	0.017
7	Olfr803	ILMN_2718049	LA weight	0.508	3.19E-07	0.019
8	Lmo3	ILMN_3139548	LA weight	0.505	3.86E-07	0.019
9	Gzmm	ILMN_1229500	LA weight	−0.495	6.99E-07	0.025
10	Ndufa1	ILMN_1251370	LA weight	−0.492	8.62E-07	0.027
11	Chrnd	ILMN_2662184	LA weight	0.483	1.39E-06	0.030
12	March4	ILMN_2793827	LA weight	0.478	1.85E-06	0.035
13	Rab6ip1	ILMN_2635232	LA weight	0.475	2.30E-06	0.038
14	2310044D20Rik	ILMN_2742739	LA weight	0.473	2.45E-06	0.038
15	Nbn	ILMN_2880745	LA weight	0.468	3.38E-06	0.043
16	Rab6ip1	ILMN_3107607	LA weight	0.466	3.64E-06	0.043
17	Tmod4	ILMN_2488846	LA weight	−0.466	3.69E-06	0.043
18	Whrn	ILMN_3082031	LA weight	−0.465	3.93E-06	0.044
19	1700001E04Rik	ILMN_2724055	LA weight	0.464	4.19E-06	0.044
20	4921505C17Rik	ILMN_2694387	LA weight	0.461	4.77E-06	0.044
21	Umps	ILMN_1254813	LA weight	0.456	6.15E-06	0.048
22	Gzmm	ILMN_1229500	Lung weight	−0.502	4.50E-07	0.020
23	Olfr1306	ILMN_3162277	Lung weight	0.490	9.53E-07	0.028
24	1110032E23Rik	ILMN_1235811	Lung weight	0.488	1.08E-06	0.029
25	Rab6ip1	ILMN_3107607	Lung weight	0.484	1.35E-06	0.030
26	Ube2e2	ILMN_2792485	Lung weight	0.463	4.34E-06	0.044
27	Rab6ip1	ILMN_2635232	Lung weight	0.462	4.55E-06	0.044
28	Adamts2	ILMN_1226259	Lung weight	0.459	5.49E-06	0.047
29	Srpx2	ILMN_2818294	Lung weight	0.457	5.93E-06	0.048

The Benjamini-Hochberg procedure with a false discovery rate of 5% was applied to account for multiple testing.

(grade II) patterns. We mapped E/A ratio and its inverse A/E ratio (in case the inverse value of the E/A ratio performs better on the linear mixed model utilized by FaST-LMM for association testing) across the HMDP on isoproterenol and identified 11 significant loci for diastolic function (**Figure 2** and **Table 2**). Mapping of left atrial weight did not yield significant loci, which could reflect isoproterenol driving the phenotype to the extreme such that there is insufficient variation to map. Here we highlight a few of the more interesting loci.

Week 0 E/A ratio mapped to a linkage disequilibrium block ($r^2 > 0.9$) around SNP rs29436095 spanning 5 genes. Of note, in a large genome-wide association meta-analysis of studies in the EchoGen consortium, E/A ratio was mapped to a statistically suggestive human locus near *Tns3* ($p = 2.11e−4$), which is syntenic to this region. The AA and GG genotypes at lead SNP rs29436095 conferred a median E/A ratio of 1.66 and 2.11, respectively. Among these genes, *Hus1* expression was downregulated with isoproterenol. *Hus1* expression under the control condition showed a trend to positive correlation with

E/A ratio (cor = 0.193, $p = 0.0867$) and mapped to the same locus as E/A ratio, indicative of a cis-eQTL that may underly the phenotype of week 0 E/A ratio. These results suggest that *Hus1* may play a role in baseline left ventricular diastolic function and is regulated with chronic isoproterenol administration.

Week 1 A/E ratio mapped to a locus near SNP rs27794930, which is in an intergenic region between *Abca1* and *Slc44a1*. Nearby SNPs in $r^2 > 0.95$ LD with the lead SNP spanned a ∼1.5 Mb window containing many genes. Among these genes, *Nipsnap3b* expression was upregulated with isoproterenol. *Nipsnap3b* expression under the control condition was positively correlated with week 1 A/E ratio (ILMN_2657376, cor = 0.32, $p = 0.004$; ILMN_2592629, cor = 0.25, $p = 0.02$) and mapped to the same locus as A/E ratio, indicative of a cis-eQTL. Our results suggest that *Nipsnap3b* may play a role in left ventricular diastolic function at week 1 of isoproterenol and is regulated by chronic isoproterenol administration. *Nipsnap3b*, which is highly expressed in skeletal muscle and heart, is a member of the NIPSNAP family with putative roles in vesicular trafficking (23, 24).
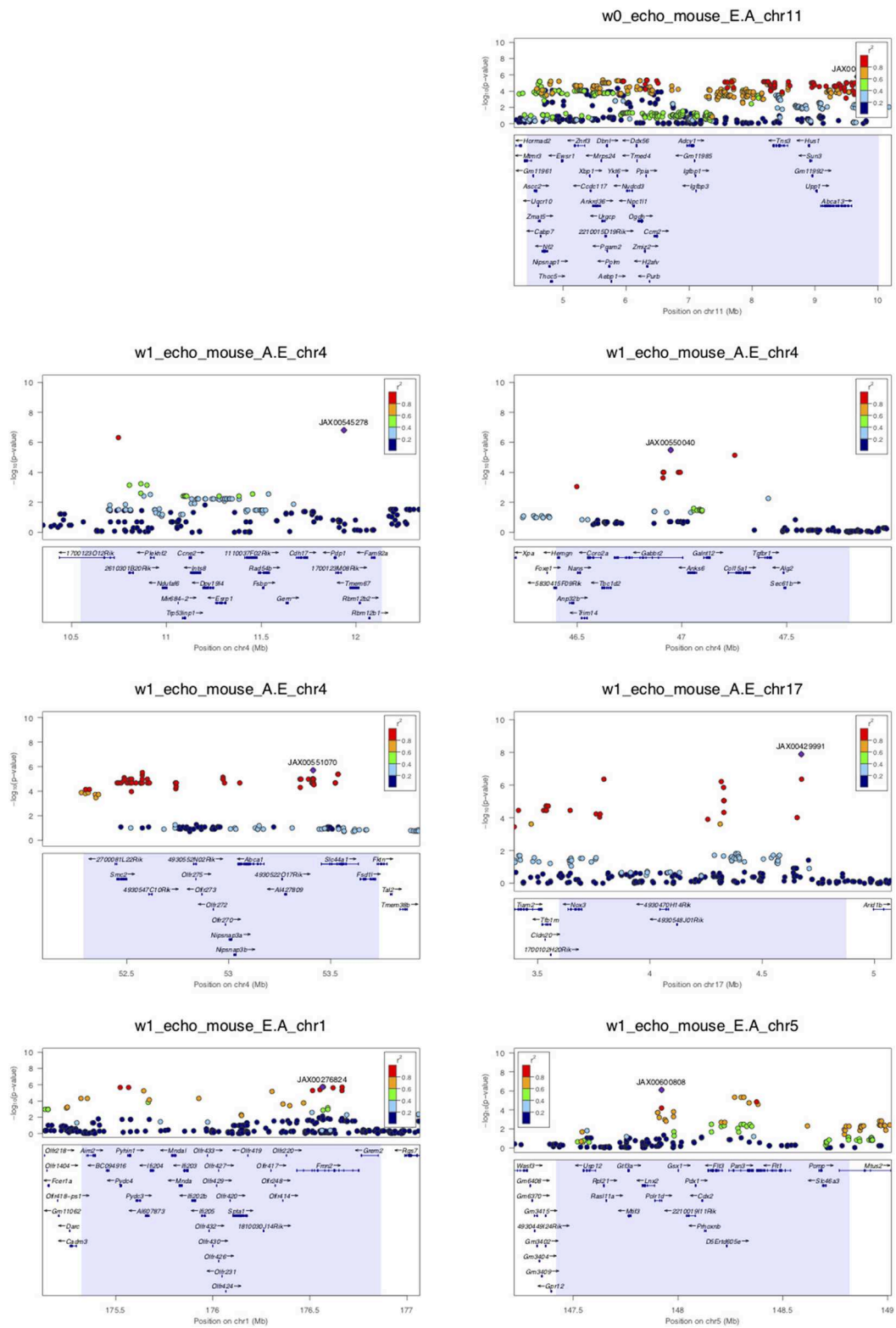
FIGURE 2 | LocusZoom plots for regional visualization of genome-wide association scan results of echocardiographic diastolic function loci. The regional lead single nucleotide polymorphism (SNP) is represented by the purple diamond symbol and annotated by its SNP ID. Surrounding SNPs are color coded according to the strength of pairwise linkage disequilibrium (LD) in terms of the r^2 metric to the lead SNP. w0, w1, w2, and w3 denote baseline, week 1, week 2, and week 3 of isoproterenol. E.A denotes E/A ratio. A.E denotes A/E ratio.

TABLE 2 | Significant echocardiographic diastolic function loci.

Analysis	Trait	Lead SNP	P-value	MAF	Genomic location of lead SNP (chr:pos)	Lead SNP type	Locus (Mb)	Candidate gene(s)	Exp	eQTL	Cor	SV
Week 0	E/A	rs29436095	1.65E-06	0.32	11:9672375	Intergenic	4.4–10.1	*Tns3*	–	–	–	M ⚡
								Hus1	8_d	Yes	Yes	–
								Sun3	–	–	–	–
								Upp1	8	Yes	No	–
								Abca13	4	No	No	MS
Week 1	E/A	rs33802297 rs33797952	1.86E-06	0.13	1:176565276-176569258	Intronic	175.3–176.9	*Fmn2* ✰	4	No	No	S
Week 1	E/A	rs32376064	7.82E-07	0.30	5:147921722	Intronic	147.4–148.9	*Lnx2*	8_d	Yes	No	–
								Polr1d ✰	–	–	–	–
								Gsx1	–	–	–	–
								Flt3	4	No	No	–
								Pan3	–	–	–	–
								Flt1	11	No	Yes	–
Week 2	E/A	rs29910955	2.69E-06	0.34	13:75682216	Intergenic	72.1–76.1	*Hnrnpa1l2-ps*	–	–	–	–
								Pcsk1	–	–	–	–
								Gm4149	–	–	–	–
								Mir682	–	–	–	–
								Ell2	4	No	No	–
								Glrx	11^d	No	Yes	–
								Rhobtb3	9	No	No	–
								Gm15528	–	–	–	–
								Gm6311	–	–	–	–
								Spata9	–	–	–	–
								Rfesd	5	No	No	–
Week 3	E/A	rs32625361	3.13E-07	0.39	4:96577960	Intergenic	96.3–98.1	*E130114P18Rik*	–	–	–	–
								Nfia	4	No	No	–
								0610025J13Rik	–	–	–	–
								Tm2d1	–	–	–	–
Week 1	A/E	rs27746189	1.54E-07	0.20	4:11936178	Exonic	10.5–12.2	*AK076817* ✰	–	–	–	
Week 1	A/E	rs27821865	3.25E-06	0.28	4:46946779	Intronic	45.6–48.9	*Gabbr2* ✰	–	–	–	
Week 1	A/E	rs27794930	1.96E-06	0.25	4:53413255	Intergenic	52.2–53.8	*Smc2*	–	–	–	MS
								Nipsnap3b	6_d	Yes	Yes	–
								Abca1	4	No	No	–
								Slc44a1	6	No	Yes	S
Week 1	A/E	rs33594278	1.29E-08	0.30	17:4674140	Intronic	3.2–4.9	*Tiam2*	5	No	No	–
								Tfb1m	–	–	–	–
								Cldn20	–	–	–	–
								Nox3	4	No	No	–
								Arid1b	–	–	–	–
								AK186662 ✰	–	–	–	–
Week 3	A/E	rs28160199	2.15E-06	0.33	4:89040388	Intronic	88.3–89.8	*Mtap*	8	No	No	M
								Cdkn2a	4	No	No	–
								Cdkn2b	–	–	–	–
								AK148321 ✰	–	–	–	–
								Dmrta1	4	No	No	–
Week 3	A/E	rs28111681 rs28096652 rs28096421	9.20E-07	0.43	4:97293373-97339169	Intronic	96.3–98.1	*Nfia* ✰	4	No	No	–

MAF denotes minor allele frequency. Locus denotes the region surrounding the lead SNP where regional SNPs are in $r^2 > 0.8$ linkage disequilibrium (LD) with the lead SNP. Candidate genes are short listed by LD cutoffs of $r^2 > 0.9$ or 0.95, if applicable. ✰ denotes the lead SNP is either intronic or exonic to the annotated gene. – Data is not available. Exp denotes approximate average $\log_2$ intensity of expression in the left ventricle, annotated by ^{d} for up- and $_d$ for down-regulation by isoproterenol. eQTL denotes the presence of cis-eQTL (p-value $< 3.63 \times 10^{-3}$) in the left ventricle. Cor denotes $p < 0.05$ for Pearson correlation between gene expression and clinical trait. SV denotes presence of structural variations among the classical inbred strains, including M for missence where SIFT score is predicted to be deleterious, S for splice region variants and ⚡ for premature stop.

Week 3 A/E ratio and E/A ratio mapped to a locus near *Nfia* (**Figure 2B**). Although there are currently no follow up data regarding the role of nuclear factor 1a in the heart, this locus has previously been associated with QRS duration on ECG, arrhythmia, and cardiomyopathy (25). Finally, week 3 A/E ratio also mapped to a locus near SNP rs28160199, which is in an intronic region of a non-coding RNA *AK148321*. Nearby SNPs in $r^2 > 0.8$ LD with the lead SNP

spanned across a region syntenic to the human 9p21 locus, containing *ANRIL*, *CDKN2A,* and *CDKN2B*, that has been associated with coronary artery disease, diabetes, and multiple cancers (26, 27).

DISCUSSION

This is the first study to genetically map diastolic function phenotypes in mice, in which a locus was found to be shared with a recent human GWAS on diastolic function. Moreover, we presented cardiac transcriptome correlation and cis-eQTL analyses that generated hypotheses regarding the involvement of the presented candidate genes and loci in the pathophysiology of diastolic dysfunction to be confirmed in follow-up basic investigations.

Recently, a large GWAS meta-analysis of echocardiographic traits, that included 46,533 individuals from 30 studies of the EchoGen consortium, evaluated 16 traits encompassing left ventricular structure, systolic and diastolic function and revealed a single significantly associated locus (28). This locus flagged by a lead intronic SNP rs12440869 on chromosome 15 near gene IQCH was found to be significantly associated with transmitral A-wave peak velocity (meta-analysis $p = 1.31e-08$). In addition, twenty-three suggestive loci for transmitral E-wave velocity, E/A ratio, deceleration time, isovolumetric relaxation time (IVR), E' velocity, E/E' velocity, diastolic dysfunction with preserved ejection function, and heart failure with preserved ejection function were reported (28). Molecular mechanisms leading to diastolic dysfunction underlying these human loci have yet to be confirmed by basic investigations. Of interest, one of the suggestive loci near *Tns3* is syntenic to a locus that week 0 E/A ratio mapped to in our study. The shared locus identified for E/A ratio suggests that a systems genetics approach in mice could be a feasible alternative in dissecting the genetic architecture of diastolic pathophysiology. Moreover, the *Tns3* locus contains many genes. We were able to prioritize *Hus1* as a putative causal gene based on cardiac tissue transcriptome correlation and cis-eQTL analyses, highlighting another benefit of studying diastolic function using the systems genetics approach in mice.

Although widely accepted in clinical practice and previously reported to accurately quantify the degree of cardiac diastolic performance in mice (13), there are a number of limitations and technical considerations worth noting regarding non-invasive assessment of diastolic function in both humans and mice. An important limitation of diastolic function assessment in mice is the difficulty in obtaining a true apical view to accurately measure mitral annular velocities by tissue Doppler. Also, diastolic function assessment in mice is somewhat complicated by a normal resting mouse heart rates at around 600 beats per minute. In the setting of excess rise, that is, heart rate > 650 bpm, due to stress of activation of the autonomic nervous system, fusion of LV filling early E and late A waves often occurs, making it difficult to assess diastolic function in mice (29). In a study examining diastolic function parameters using multiple mouse models of heart disease, mitral E/A

ratio assessment was noted to be technically difficult due to high heart rates; combined measurement of left atrial area and reverse longitudinal strain rate and/or isovolumic relaxation time (IVRT) was felt to be necessary for an overall assessment of diastolic function (30). A major limitation of our study is that, at the time of our echocardiographic assessment, tissue Doppler velocity and longitudinal strain rate were not yet available. We relied on the ratio of mitral inflow E and A velocities, which is invariant to Doppler interrogation angle, as our primary echocardiographic measure of diastolic function for genome mapping. Thus, future diastolic assessment incorporating additional measures may more accurately capture the phenotype of interest.

Finally, diastolic function is a product of environmental, genetic, and co-morbid factors in humans and non-invasive parameters of diastolic function assessment are subjected to changes in loading conditions that may be difficult to control in both humans and mice, even under well-defined experimental settings. Quantitative measures of diastolic function that reflect intrinsic elastance, such as end diastolic pressure-volume relationship (EDPVR) and end systolic pressure-volume relationship (ESPVR) derived from invasive hemodynamic monitoring under different loading conditions, are robust and may significantly increase mapping power and accuracy. We hypothesize that genetic mapping of invasive measurements of left ventricular intrinsic elastance in a genetically diverse population, such as the HMDP, will significantly improve the accuracy of mapping for various models of diastolic dysfunction, such as aging and obesity, and accelerate the understanding of diastolic pathophysiology in mice and humans.

DATA AVAILABILITY

Publicly available datasets were analyzed in this study. This data can be found here: https://www.ncbi.nlm.nih.gov/geo/query/acc.cgi?acc=GSE48760.

ETHICS STATEMENT

All animal experiments were conducted following guidelines established and approved by the University of California, Los Angeles Institutional Animal Care and Use Committee. This study was carried out in accordance with the recommendations of the University of California, Los Angeles Institutional Animal Care and Use Committee. The protocol was approved by the University of California, Los Angeles Institutional Animal Care and Use Committee.

AUTHOR CONTRIBUTIONS

JW, YW, and AL contributed to conception and design of the study. JW performed echocardiograms, measured diastolic parameters, prepared samples for RNA isolation, organized the data, performed statistical analysis, and drafted the manuscript. AH-V provided critical revisions for important intellectual

content of the manuscript. YW and AL provided critical feedback and mentorship. All authors contributed to manuscript revision and approved the submitted version.

SUPPLEMENTARY MATERIAL

The Supplementary Material for this article can be found online at: https://www.frontiersin.org/articles/10.3389/fcvm.2019.00100/full#supplementary-material

REFERENCES

1. Yancy CW, Jessup M, Bozkurt B, Butler J, Casey DE, Jr, Drazner MH, et al. 2013 ACCF/AHA guideline for the management of heart failure: a report of the American College of Cardiology Foundation/American Heart Association Task Force on Practice Guidelines. *J Am Coll Cardiol.* (2013) 62:e147–239. doi: 10.1016/j.jacc.2013.05.019

2. Halley CM, Houghtaling PL, Khalil MK, Thomas JD, Jaber WA. Mortality rate in patients with diastolic dysfunction and normal systolic function. *Arch Intern Med.* (2011) 171:1082–7. doi: 10.1001/archinternmed.2011.244

3. Gharacholou SM, Scott CG, Takahashi PY, Nkomo VT, McCully RB, Fine NM, et al. Left ventricular diastolic function and long-term outcomes in patients with normal exercise echocardiographic findings. *Am J Cardiol.* (2013) 112:200–7. doi: 10.1016/j.amjcard.2013.03.009

4. Aljaroudi W, Alraies MC, Halley C, Rodriguez L, Grimm RA, Thomas JD, et al. Impact of progression of diastolic dysfunction on mortality in patients with normal ejection fraction. *Circulation.* (2012) 125:782–8. doi: 10.1161/CIRCULATIONAHA.111.066423

5. Mozaffarian D, Benjamin EJ, Go AS, Arnett DK, Blaha MJ, Cushman M, et al. Heart disease and stroke statistics−2015 update: a report from the American Heart Association. *Circulation.* (2015) 131:e29–322.

6. Yancy CW, Jessup M, Bozkurt B, Butler J, Casey DE, Jr, Colvin MM, et al. 2017 ACC/AHA/HFSA Focused Update of the 2013 ACCF/AHA Guideline for the Management of Heart Failure: a report of the American college of cardiology/american heart association task force on clinical practice guidelines and the heart failure society of America. *J Card Fail.* (2017) 23:628–51.

7. Lusis AJ, Seldin MM, Allayee H, Bennett BJ, Civelek M, Davis RC, et al. The hybrid mouse diversity panel: a resource for systems genetics analyses of metabolic and cardiovascular traits. *J Lipid Res.* (2016) 57:925–42. doi: 10.1194/jlr.R066944

8. Rau CD, Romay MC, Tuteryan M, Wang JJ, Santolini M, Ren S, et al. Systems genetics approach identifies gene pathways and Adamts2 as drivers of isoproterenol-induced cardiac hypertrophy and cardiomyopathy in mice. *Cell Syst.* (2017) 4:121–8 e4. doi: 10.1016/j.cels.2016.10.016

9. Rau CD, Wang J, Avetisyan R, Romay MC, Martin L, Ren S, et al. Mapping genetic contributions to cardiac pathology induced by Beta-adrenergic stimulation in mice. *Circ Cardiovasc Genet.* (2015) 8:40–9. doi: 10.1161/CIRCGENETICS.113.000732

10. Wang JJ, Rau C, Avetisyan R, Ren S, Romay MC, Stolin G, et al. Genetic dissection of cardiac remodeling in an isoproterenol-induced heart failure mouse model. *PLoS Genet.* (2016) 12:e1006038. doi: 10.1371/journal.pgen.1006038

11. Brooks WW, Conrad CH. Isoproterenol-induced myocardial injury and diastolic dysfunction in mice: structural and functional correlates. *Comp Med.* (2009) 59:339–43.

12. Brutsaert DL, Sys SU, Gillebert TC. Diastolic failure: pathophysiology and therapeutic implications. *J Am Coll Cardiol.* (1993) 22:318–25. doi: 10.1016/0735-1097(93)90850-Z

13. Respress JL, Wehrens XH. Transthoracic echocardiography in mice. *J Vis Exp.* (2010) 39:1738. doi: 10.3791/1738

14. Yang H, Ding Y, Hutchins LN, Szatkiewicz J, Bell TA, Paigen BJ, et al. A customized and versatile high-density genotyping array for the mouse. *Nat Methods.* (2009) 6:663–6. doi: 10.1038/nmeth.1359

15. Lippert C, Listgarten J, Liu Y, Kadie CM, Davidson RI, Heckerman D. FaST linear mixed models for genome-wide association studies. *Nat Methods.* (2011) 8:833–5. doi: 10.1038/nmeth.1681

16. Langfelder P, Horvath S. WGCNA: an R package for weighted correlation network analysis. *BMC Bioinform.* (2008) 9:559. doi: 10.1186/1471-2105-9-559

17. Nagueh SF, Appleton CP, Gillebert TC, Marino PN, Oh JK, Smiseth OA, et al. Recommendations for the evaluation of left ventricular diastolic function by echocardiography. *J Am Soc Echocardiogr.* (2009) 22:107–33. doi: 10.1016/j.echo.2008.11.023

18. Wang X, Chen W, Zhang J, Khan A, Li L, Huang F, et al. Critical role of ADAMTS2 (A Disintegrin and Metalloproteinase With Thrombospondin Motifs 2) in Cardiac Hypertrophy Induced by Pressure Overload. *Hypertension.* (2017) 69:1060–9. doi: 10.1161/HYPERTENSIONAHA.116.08581

19. Sauzeau V, Jerkic M, Lopez-Novoa JM, Bustelo XR. Loss of Vav2 proto-oncogene causes tachycardia and cardiovascular disease in mice. *Mol Biol Cell.* (2007) 18:943–52. doi: 10.1091/mbc.e06-09-0877

20. Gokhin DS, Lewis RA, McKeown CR, Nowak RB, Kim NE, Littlefield RS, et al. Tropomodulin isoforms regulate thin filament pointed-end capping and skeletal muscle physiology. *J Cell Biol.* (2010) 189:95–109. doi: 10.1083/jcb.201001125

21. Zhang QJ, Tran TAT, Wang M, Ranek MJ, Kokkonen-Simon KM, Gao J, et al. Histone lysine dimethyl-demethylase KDM3A controls pathological cardiac hypertrophy and fibrosis. *Nat Commun.* (2018) 9:5230. doi: 10.1038/s41467-018-07173-2

22. Luther DJ, Thodeti CK, Shamhart PE, Adapala RK, Hodnichak C, Weihrauch D, et al. Absence of type VI collagen paradoxically improves cardiac function, structure, and remodeling after myocardial infarction. *Circ Res.* (2012) 110:851–6. doi: 10.1161/CIRCRESAHA.111.252734

23. Buechler C, Bodzioch M, Bared SM, Sigruener A, Boettcher A, Lapicka-Bodzioch K, et al. Expression pattern and raft association of NIPSNAP3 and NIPSNAP4, highly homologous proteins encoded by genes in close proximity to the ATP-binding cassette transporter A1. *Genomics.* (2004) 83:1116–24. doi: 10.1016/j.ygeno.2003.12.011

24. Consortium GT. The Genotype-Tissue Expression (GTEx) project. *Nat Genet.* (2013) 45:580–5.

25. Ritchie MD, Denny JC, Zuvich RL, Crawford DC, Schildcrout JS, Bastarache L, et al. Genome- and phenome-wide analyses of cardiac conduction identifies markers of arrhythmia risk. *Circulation.* (2013) 127:1377–85. doi: 10.1161/CIRCULATIONAHA.112.000604

26. Congrains A, Kamide K, Ohishi M, Rakugi H. ANRIL: Molecular mechanisms and implications in human health. *Int J Mol Sci.* (2013) 14:1278–92. doi: 10.3390/ijms14011278

27. Holdt LM, Teupser D. Long Noncoding RNA ANRIL: Lnc-ing genetic variation at the chromosome 9p21 locus to molecular mechanisms of Atherosclerosis. *Front Cardiovasc Med.* (2018) 5:145. doi: 10.3389/fcvm.2018.00145

28. Wild PS, Felix JF, Schillert A, Teumer A, Chen MH, Leening MJG, et al. Large-scale genome-wide analysis identifies genetic variants associated

with cardiac structure and function. *J Clin Invest.* (2017) 127:1798–812. doi: 10.1172/JCI84840

29. Lindsey ML, Kassiri Z, Virag JAI, de Castro Bras LE, Scherrer-Crosbie M. Guidelines for measuring cardiac physiology in mice. *Am J Physiol Heart Circ Physiol.* (2018) 314:H733–H52. doi: 10.1152/ajpheart.00 339.2017

30. Schnelle M, Catibog N, Zhang M, Nabeebaccus AA, Anderson G, Richards DA, et al. Echocardiographic evaluation of diastolic function in mouse models of heart disease. *J Mol Cell Cardiol.* (2018) 114:20–8. doi: 10.1016/j.yjmcc.2017. 10.006

Conflict of Interest Statement: The authors declare that the research was conducted in the absence of any commercial or financial relationships that could be construed as a potential conflict of interest.